State-To-State Integral Cross Section for the $H + H_2O \rightarrow H_2 + OH$ Abstraction Reaction

Dong H. Zhang,* Daiqian Xie, and Minghui Yang
Department of Computational Science, The National University of Singapore, Singapore, 119260

Soo-Y. Lee
Department of Chemistry, The National University of Singapore, Singapore, 119260
(Received 3 September 2002; published 27 December 2002)

The initial state selected time-dependent wave-packet method was extended to calculate the state-to-state integral cross section for the title reaction with H_2O in the ground rovibrational state on the potential energy surface of Yang, Zhang, Collins, and Lee. One OH bond length was fixed in the study, which is justifiable for the abstraction reaction, but the remaining 5 degrees of freedom were treated exactly. It was found that the H_2 molecule is produced vibrationally cold for collision energy up to 1.6 eV. The OH rotation takes away about 4% of total available energy in the products, while the fraction of energy going to H_2 rotation increases with collision energy to about 20% at 1.6 eV.

DOI: 10.1103/PhysRevLett.89.283203 PACS numbers: 34.50.Lf, 34.20.Mq

The state-to-state differential cross sections provide the most detailed information on a chemical reaction available experimentally, and the ability to calculate them accurately has long been the goal of the theoretical dynamicist. The first converged calculations of cross sections for a chemical reaction were reported for the $H + H_2$ reaction in 1976 [1]. It took over ten years before accurate results for reactions more complicated than this were computed, with the development of the new quantum scattering theories and modern computer technology [2,3].

Once the atom-diatom reactive scattering problem had essentially been solved, attention naturally turned to more complicated reactions involving more than three atoms. In the last decade, significant progress in quantum mechanical studies of four-atom chemical reactions was made [4–21]. Starting from reduced dimensionality approaches [22,23], it is now possible to calculate fully converged integral cross sections [14,16–21], as well as full-dimensional state-to-state reaction probabilities for the total angular momentum $J = 0$ [8–11] without any dynamical approximations, mainly through the development of the initial state selected wave-packet method [4,5,7,14,20]. This development has combined with the advances for constructing potential energy surfaces [24], and with the rise in computational power to make accurate *ab initio* dynamics practical for four-atom systems [15–18].

Despite this significant progress, the accurate quantum calculation of the *state-to-state* integral or differential cross sections for four-atom reactions remained a challenge. Up to now, all the state-to-state cross sections for four-atom reactions were calculated by using either the reduced dimensionality method or quasiclassical simulations. There have been some full-dimensional state-to-state dynamics calculations on the benchmark $H + H_2O \leftrightarrow H_2 + OH$ reaction, but they were all limited to total angular momentum $J = 0$. Advancing from $J = 0$ to $J > 0$ has proven to be extremely difficult due to the rapid increase of the rotational basis functions needed in calculation.

In this Letter, we report the first five dimensional (5D) *state-to-state* integral cross sections (ICS) for the $H + H_2O \rightarrow H_2(v_1, j_1) + OH(j_2)$ reaction for the initial ground rovibrational state. The $H + H_2O$ and its isotopically substituted reactions have become the prototype for tetra-atomic reactions, in much the same way that the $H + H_2$ reaction served as the prototype for triatomics. They may be the simplest systems in which there are different vibrational modes in the reactants which can play an important role in the reaction dynamics. The reverse reaction, $H_2 + OH \rightarrow H + H_2O$, is an extremely important reaction in combustion. Theoretically, because three of the four atoms are hydrogens, the system is an ideal candidate for pursuing both high quality *ab initio* calculation of a potential energy surface (PES) and accurate quantum reactive scattering calculations. The construction of a global PES of a quantitative accuracy recently [16,25] and extensive dynamics studies of the reaction on the PES have made it the first four-atom reaction system studied at a quantitative level.

The time-dependent wave-packet method has been used to calculate the first state-to-state reaction probabilities for $J = 0$ for the title reaction [8]. In the present study, we extended the method to calculate the state-to-state reaction probabilities for $J > 0$ from which the state-to-state cross sections were obtained. We employed the potential energy surface of Yang, Zhang, Collins, and Lee (YZCL2 PES) in our dynamics calculation because it is the most accurate PES available [25]. We fixed one OH bond length in the H_2O reactant, but treated the remaining 5 degrees of freedom exactly. It has been shown in our recent studies [19,20] that one OH bond in the H_2O reactant can be treated very well as a spectator bond,

and can even be frozen in studying the $H + H_2O \rightarrow H_2 + OH$ abstraction reaction; however, both OH bonds should be treated as reactive bonds in studying the $H' + H_2O \rightarrow HOH' + H$ exchange reaction. Thus freezing the OH bond is expected to be a good approximation for studying the state-to-state integral cross section for the abstraction reaction. We propagated an initial wave packet for the H_2O reagent in the initial ground rovibrational state in the atom-triatom coordinates from the asymptotic region to $R_{13} = 6.0a_0$. It is straightforward to carry out this propagation, because at that R_{13} distance the projection of the total angular momentum on the body fixed axis, K, for the wave packet remains at zero exclusively even for a large J initial state. A coordinate transformation was then carried out to transfer the wave packet from the atom-triatom coordinates to diatom-diatom coordinates. After the transformation, we propagated the wave packet in the diatom-diatom coordinates as in Ref. [7] by including all important K components. We used the parameters in Ref. [20] to propagate the initial wave packet in the atom-triatom coordinates. In the diatom-diatom coordinates, we used a total number of 178 sine functions (among them 48 for the interaction region) for the translational coordinate R in the range $[0.2, 15.5]a_0$. A total of 60 vibrational functions are employed in the range $[0.7, 9.0]a_0$ for the reagent H_2. For the rotational part, we used $j_{1\max} = 50$ for H_2, $j_{2\max} = 18$ for OH, which roughly results in 8000 rotational basis functions for $K > 0$. We included up to 15 K blocks to fully converge the state-to-state reaction probability. Thus the largest total rotational basis reaches 110 000. Since the bond length for the nonreactive OH was frozen, the final state-to-state integral cross section depends only on v_1, j_1, j_2, and is denoted by $\sigma(v_1, j_1, j_2)$.

Figure 1 shows the total cross section, $\sigma = \sum_{v_1,j_1,j_2} \sigma(v_1, j_1, j_2)$, and the H_2 vibrational state resolved cross sections, $\sigma(v_1) = \sum_{j_1,j_2} \sigma(v_1, j_1, j_2)$, as a function of translational energy. Also shown (in crosses) is the fully converged total cross section calculated in the atom-triatom coordinates with one OH bond frozen [20]. As can be seen, the agreement between these two ICS is perfect although the current ICS has been calculated via a much more complicated sum over partial cross sections. In the energy region considered in this study, there is only a small fraction of $H_2(v = 1)$ produced, with a population of 3.3% at $E = 1.6$ eV. The $H_2(v = 2)$ is energetically open at $E = 1.38$ eV, but the population is totally negligible in the energy region considered here. Since the OH bond length was frozen in this study, we are not able to obtain the population of OH product in the vibrationally excited states. But, we find from a full-dimensional calculation of the state-to-state reaction probability for $J = 0$ that the fraction of OH vibrationally excited population is extremely small [26]. Hence, we can conclude that in the energy region considered here both H_2 and OH products are vibrationally very cold.

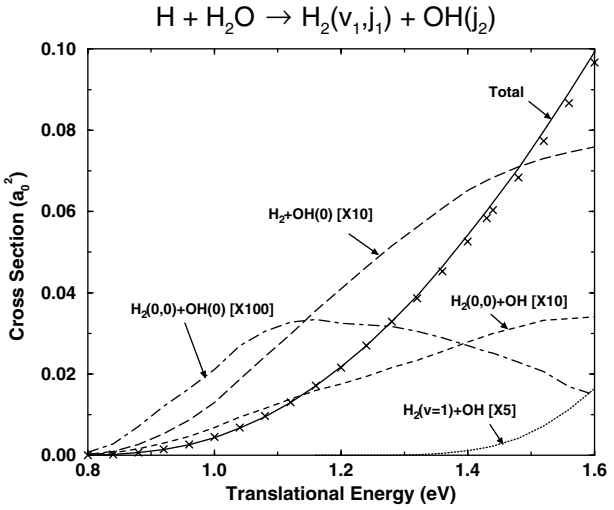

FIG. 1. Total and final vibrational/rotational state specific integral cross sections for the $H + H_2O \rightarrow H_2 + OH$ reaction as a function of translational energy. The total cross sections in crosses were calculated in the atom-triatom coordinates [20].

Also shown in Fig. 1 are the ICS for both H_2 and OH products, or one of the products, in the ground rovibrational state. The ICS for the $H_2(v = 0, j_1 = 0) + OH(j_2 = 0)$ products, $\sigma(v_1 = 0, j_1 = 0, j_2 = 0)$, is multiplied by a factor of 100 before plotting. It increases with the increase of translational energy in the low energy region, but slower than the increase of the total cross section. At $E = 1.15$ eV, it reaches a maximum, and then begins to decrease gradually with the further increase of translational energy. The ICS for either H_2 or OH product in the ground rovibrational state is multiplied by a factor of 10 before plotting. As can be seen, the ICS for the $H_2 + OH(j_2 = 0)$ products, $\sigma(j_2 = 0) = \sum_{v_1,j_1} \sigma(v_1, j_1, j_2 = 0)$, is larger than that for the $H_2(v = 0, j_1 = 0) + OH$ products, $\sigma(v_1 = 0, j_1 = 0) = \sum_{j_2} \sigma(v_1 = 0, j_1 = 0, j_2)$, by about a factor of 2. This means that the probability to produce OH in the ground rovibrational state is about a factor of 2 larger than that to produce H_2 in the ground rovibrational state, or the probability to produce H_2 in rotationally excited states is larger than that to produce OH in rotationally excited states, despite the fact that the OH rotational constant is smaller than that for H_2 by a factor of 3. This is because the torque for OH rotation is small for the reaction.

In Fig. 2, we present ICS to specific final rotational states of either H_2 [Fig. 2(a)] or OH [Fig. 2(b)] product, and relative population for rotational states of either H_2 [Fig. 2(c)] or OH [Fig. 2(d)] product, at several values of energy. As can be seen from Fig. 2(b), $\sigma(j_2) = \sum_{v_1,j_1} \sigma(v_1, j_1, j_2)$ has a maximum at $j_2 = 2$ for all the energies shown [except $E = 1.0$ eV for which $\sigma(j_2 = 0)$ is marginally larger than $\sigma(j_2 = 2)$]. In contrast, the most probable rotational state for H_2 becomes higher with the increase of translational energy as shown in Fig. 2(a). The

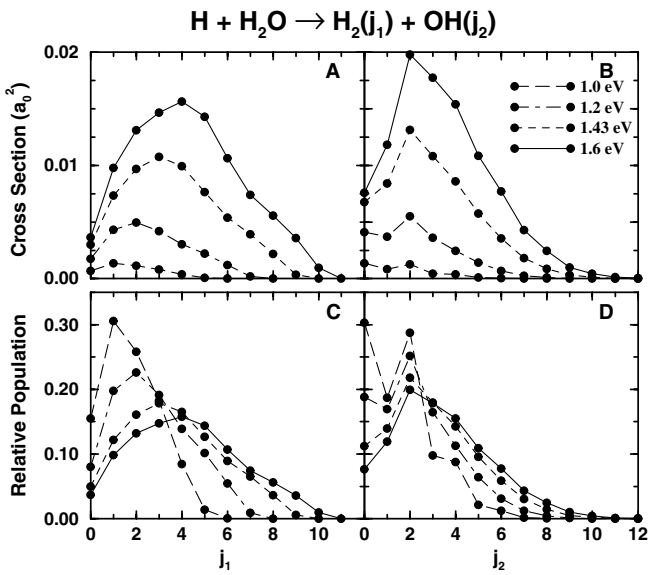

FIG. 2. Integral cross sections to specific final rotational states of either (A) H_2 or (B) OH product, and relative population for rotational states of either (C) H_2 or (D) OH product, at $E = 1.0$, 1.2, 1.43, 1.60 eV.

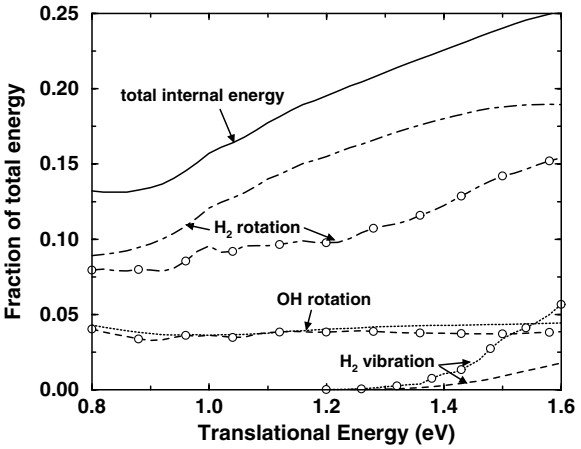

FIG. 3. The fraction of the total available energy in product channel going into rovibration of H_2 and rotation of OH as a function of translational energy calculated from state-to-state integral cross sections (curves without any symbols) and from $J = 0$ state-to-state reaction probability (with open circles).

general trend in the change of H_2 or OH relative population with an increase of translational energy is quite similar—the distribution becomes broader, and the $j_1 = 0$ or $j_2 = 0$ population declines; in particular, the j_2 population decreases from 30% at $E = 1.00$ to less than 10% at $E = 1.60$ eV. The OH rotational distribution at $E = 1.00$ eV is rather oscillatory, with a maximum at $j_2 = 0$. Furthermore, it can be seen that the populations for even OH rotational states are substantially larger than those for adjacent higher odd OH rotational states.

The difference in the rotational excitation of H_2 and OH can also be found from the fraction of the total available energy in the product channel going into rotations of H_2 and OH. Figure 3 shows the fractions of the total available energy in the product channel going into rotations of H_2 and OH, as well as vibration of H_2. Also shown in the figure (with open circles) are the fractions calculated from the state-to-state reaction probability for $J = 0$. For the energy region considered here, only a very small fraction of the available energy goes into H_2 vibration. At $E = 1.6$ eV, it reaches only 1.7%, although it steadily increases with the increase of collision energy. The fraction of energy going into OH rotation essentially does not change with the collision energy. It remains around 4% in the energy region considered. In contrast, the fraction of total available energy going to H_2 rotation steadily increases from a value of 9% at $E = 0.8$ eV to a value of 20% at $E = 1.6$ eV. Thus the H_2 rotation takes away considerably more energy than OH rotation, and the difference increases with the increase of collision energy. The overall fraction of collision energy going into internal rovibrational motion of the products is low. It increases from 13% at $E = 0.8$ eV to a little more than 25% at $E = 1.6$ eV. So, most of the available energy in this reaction goes into the translational motion of the products.

The fractions of energy going into internal motion of the products discussed so far were obtained from the state-to-state ICS which includes the contributions from all the important $J \geq 0$ state-to-state reaction probabilities. For each $J \geq 0$ state-to-state reaction probability, we can also calculate such fractions. Sometimes, we simply use the fractions obtained from the $J = 0$ reaction probability to approximately study the distribution of total available energy among the products. As can be seen from Fig. 3, only for OH rotation is the fraction obtained from the $J = 0$ reaction probability close to that obtained from ICS, with the former slightly lower than the latter. For the H_2 rotation, the fraction obtained from ICS is considerably larger than that obtained from the $J = 0$ reaction probability, with the largest difference of about 40% around $E = 1.2$ eV. For H_2 vibration, the difference is even bigger. The fraction obtained from the $J = 0$ reaction probability is about a factor of 3 larger than that obtained from ICS. The differences between the fraction of energy going into H_2 rotation and vibration obtained from ICS and that obtained from $J = 0$ reaction probability clearly reveal that as J (impact parameter) increases, the H_2 molecule is produced rotationally hotter, while vibrationally much cooler. This is true for a reaction with a collinear saddle geometry, as for this reaction. Hence one should be cautious in handling the final state distributions or product energy distributions obtained from the $J = 0$ reaction probability.

Finally, it is interesting to see if there is any correlation between $H_2(v_1 = 0)$ and OH rotations from the average H_2 rotation quantum number associated with different

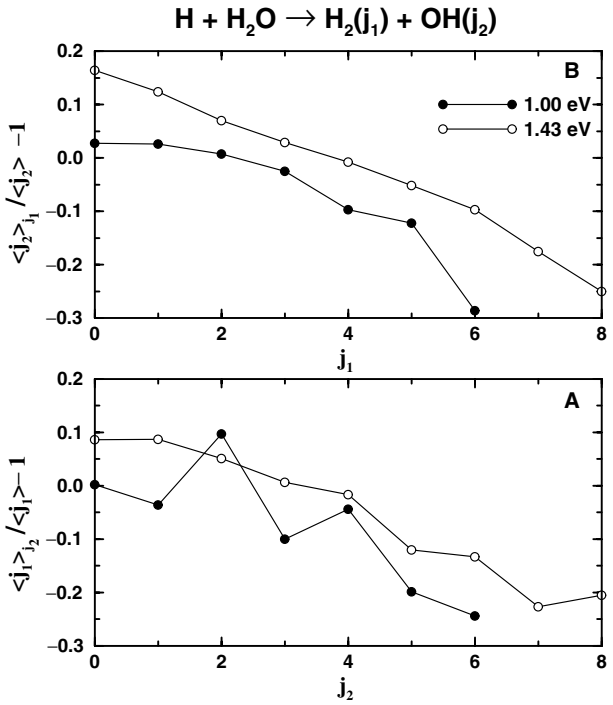

FIG. 4. Difference between the average H_2 (OH) rotation quantum number associated with different OH (H_2) rotational states and the overall average rotation quantum number of H_2 (OH) as a function of OH (H_2) rotation.

OH rotational states, $\langle j_1\rangle_{j_2}$, and the average OH rotation quantum number associated with different H_2 rotational states, $\langle j_2\rangle_{j_1}$. If there is no correlation between H_2 and OH rotations, $\langle j_1\rangle_{j_2}$ ($\langle j_2\rangle_{j_1}$) should be equal to the overall average rotation quantum number for H_2 (OH), $\langle j_1\rangle$ ($\langle j_2\rangle$). Thus the difference between $\langle j_1\rangle_{j_2}$ ($\langle j_2\rangle_{j_1}$) and $\langle j_1\rangle$ ($\langle j_2\rangle$) can give a clear measurement of the correlation between the H_2 and OH rotations. As can be seen from $\langle j_1\rangle_{j_2}/\langle j_1\rangle - 1$ [Fig. 4(a)] and $\langle j_2\rangle_{j_1}/\langle j_2\rangle - 1$ [Fig. 4(b)] for $E = 1.0$ and 1.43 eV, $H_2(v_1 = 0)$ and OH rotations are correlated to some extent. The value of $\langle j_2\rangle_{j_1}/\langle j_2\rangle - 1$ decreases monotonically from a positive value to a negative value with the increase of j_1 [Fig. 4(b)]. This shows that with the increase of j_1, the average value of j_2 decreases. The value of $\langle j_1\rangle_{j_2}/\langle j_1\rangle - 1$ at $E = 1.43$ eV shown in Fig. 4(a) also decreases with j_2. However, the dependence of $\langle j_1\rangle_{j_2}/\langle j_1\rangle - 1$ with j_2 at $E = 1.0$ eV shown in Fig. 4(a) shows some oscillatory structures, in strong correlation with the OH rotational state distribution at that energy shown in Fig. 2(d). The even OH rotational states have larger j_1 average values and larger populations than the adjacent odd OH rotational states, in particular, for $j_2 = 2$ state. However, this propensity diminishes with the increase of collision energy.

Comparisons between our results with available experimental results and other theoretical results obtained mainly by using quasiclassical trajectory method on the YZCL2 PES, as well as on other PES, will be pursued in a follow-up work.

This work is supported in part by an academic research grant from Ministry of Education and Agency for Science, Technology and Research, Republic of Singapore.

*Electronic address: zhangdh@cz3.nus.edu.sg

[1] G. C. Schatz and A. Kupperman, J. Chem. Phys. **65**, 4668 (1976).
[2] G. C. Schatz, Annu. Rev. Phys. Chem. **39**, 317 (1988).
[3] W. H. Miller, Annu. Rev. Phys. Chem. **41**, 245 (1990).
[4] D. H. Zhang and J. Z. H. Zhang, J. Chem. Phys. **101**, 1146 (1994).
[5] D. Neuhauser, J. Chem. Phys. **100**, 9272 (1994).
[6] U. Manthe, T. Seideman, and W. H. Miller, J. Chem. Phys. **99**, 10 078 (1993).
[7] D. H. Zhang and J. C. Light, J. Chem. Phys. **104**, 4544 (1996).
[8] D. H. Zhang and J. C. Light, J. Chem. Phys. **105**, 1291 (1996).
[9] W. Zhu, J. Dai, J. Z. H. Zhang, and D. H. Zhang, J. Chem. Phys. **105**, 4881 (1996).
[10] J. Dai, W. Zhu, and J. Z. H. Zhang, J. Phys. Chem. **100**, 13 901 (1996).
[11] S. K. Pogrebnya, J. Echave, and D. C. Clary, J. Chem. Phys. **107**, 8975 (1997).
[12] F. Matzkies and U. Manthe, J. Chem. Phys. **108**, 4828 (1998).
[13] D. H. Zhang, J. C. Light, and S. Y. Lee, J. Chem. Phys. **109**, 79 (1998).
[14] D. H. Zhang and S. Y. Lee, J. Chem. Phys. **110**, 4435 (1999).
[15] D. H. Zhang, M. A. Collins, and S.-Y. Lee, Science **290**, 961 (2000).
[16] M. Yang, D. H. Zhang, M. A. Collins, and S.-Y. Lee, J. Chem. Phys. **114**, 4759 (2001).
[17] D. H. Zhang, M. Yang, and S.-Y. Lee, J. Chem. Phys. **114**, 8733 (2001).
[18] D. H. Zhang, M. Yang, and S.-Y. Lee, J. Chem. Phys. **116**, 2388 (2002).
[19] D. H. Zhang, M. Yang, and S.-Y. Lee, Phys. Rev. Lett. **89**, 103201 (2002).
[20] D. H. Zhang, M. Yang, and S.-Y. Lee, J. Chem. Phys. (to be published).
[21] E. M. Goldfield and S. K. Gray, J. Chem. Phys. **117**, 1604 (2002).
[22] D. C. Clary, J. Phys. Chem. **98**, 10 678 (1994).
[23] J. M. Bowman and G. C. Schatz, Annu. Rev. Phys. Chem. **46**, 169 (1996).
[24] R. P. A. Bettens and M. A. Collins, J. Chem. Phys. **111**, 816 (1999).
[25] M. Yang, D. H. Zhang, M. A. Collins, and S.-Y. Lee, J. Chem. Phys. **115**, 174 (2001).
[26] D. H. Zhang, D. Xie, M. Yang, and S.-Y. Lee (unpublished).